Published in final edited form as:

Sci Transl Med. 2017 March 15; 9(381): . doi:10.1126/scitranslmed.aai7521.

Mimicry of an HIV broadly neutralizing antibody epitope with a synthetic glycopeptide

S. Munir Alam[1,2,3,*,†], **Baptiste Aussedat**[4,†], **Yusuf Vohra**[4,†], **R. Ryan Meyerhoff**[1,5,†], **Evan M. Cale**[6,†], **William E. Walkowicz**[4,†], **Nathan A. Radakovich**[6], **Kara Anasti**[1], **Lawrence Armand**[1], **Robert Parks**[1], **Laura Sutherland**[1], **Richard Scearce**[1], **M. Gordon Joyce**[6], **Marie Pancera**[6], **Aliaksandr Druz**[6], **Ivelin S. Georgiev**[6], **Tarra Von Holle**[1], **Amanda Eaton**[1], **Christopher Fox**[7], **Steven G. Reed**[7], **Mark Louder**[6], **Robert T. Bailer**[6], **Lynn Morris**[8,9], **Salim S. Abdool-Karim**[8,9], **Myron Cohen**[10], **Hua-Xin Liao**[1,2,‡], **David C. Montefiori**[1,2,11], **Peter K. Park**[4], **Alberto Fernández-Tejada**[4], **Kevin Wiehe**[1], **Sampa Santra**[12], **Thomas B. Kepler**[13], **Kevin O.**

[*]Corresponding author: barton.haynes@dm.duke.edu (B.F.H.); munir.alam@dm.duke.edu (S.M.A.).
[†]These authors contributed equally to this work.
[‡]Present address: College of Life Science and Technology, Jinan University, Guangzhou 510632, China.

SUPPLEMENTARY MATERIALS
www.sciencetranslationalmedicine.org/cgi/content/full/9/381/eaai7521/DC1
Supplementary Text.
Fig. S1. Man9-V3 glycopeptide binding to glycan-dependent V3 bnAbs.
Fig. S2. PGT128-like specificity in HIV-1–chronically infected donor CH765.
Fig. S3. Sort gates to isolate V3-glycan bnAbs from HIV-1–infected donor CH765.
Fig. S4. Epitope mapping of newly isolated V3-glycan mAbs.
Fig. S5. Binding of DH563-VRC41 V3-glycan bnAb family to Man9-V3 and aglycone V3.
Fig. S6. Autoreactivity of newly isolated V3-glycan mAbs.
Fig. S7. Affinity measurement of V3 bnAb binding to Man9-V3 glycopeptide.
Fig. S8. Affinity measurements of isolated V3-glycan bnAbs to BG505 SOSIP trimers.
Fig. S9. Neutralization of V3-glycan bnAbs against a diverse panel of viruses.
Fig. S10. Flow cytometry sort gates to isolate DH706-DH710 from Man9-V3 immunized macaques.
Fig. S11. Binding of vaccine-induced antibodies isolated from Man9-V3 immunized rhesus macaques to HIV-1 antigens.
Table S1. Immunogenetics of DH563-VRC41 V3-glycan bnAb family.
Table S2. Neutralization of N^{332}-dependent mAbs isolated with Man9-V3 glycopeptide and native-like SOSIP trimers.
Table S3. Immunogenetics of vaccine-induced antibodies isolated from Man9-V3 immunized rhesus macaques.
Data set S1. Mass spectrophotometry spectra for Man9-V3 and synthetic intermediates.
Data set S2. IC_{50} and IC_{80} neutralization values for V3-glycan bnAbs against a diverse panel of HIV-1 Env pseudoviruses.
Data set S3. Primers used to amplify DH563 Ig genes.
References (40, 41)

Author contributions: S.M.A., R.R.M., E.M.C., Y.V., B.A., and B.F.H. wrote and edited the paper. B.F.H. and J.S. designed the glycopeptide; B.F.H. analyzed all data, wrote and edited the paper, and directed all aspects of the study. M.B. provided intellectual contribution to the study. Y.V., B.A., W.E.W., P.K.P., A.F.-T., and S.D. synthesized and purified peptides and glycans. L.A. and M.A.M. produced the tetramerized and fluorophore-conjugated glycopeptide. M.G.J., M.P., A.D., and I.S.G. designed and produced the SOSIP trimers. K.A. performed BLI, and R.R.M. and R.P. performed ELISA binding antibody assays. K.O.S. performed the glycan array analysis. R.R.M., E.M.C., and N.A.R. performed single-cell sorting and characterization of isolated antibodies. P.D.K. directed the production of SOSIP probes, and J.R.M. directed the isolation and characterization of CH765-VRC41.01 and CH765-VRC41.02. H.-X.L. directed the production and purification of Env proteins. K.W. and T.B.K. directed computational analysis of antibody lineages. T.V.H. performed HEp-2 cell staining. A.E., D.C.M., R.T.B., and M.L. directed mAb and serum neutralization studies. L.S., S.S., and R.S. directed immunization of rhesus macaques. C.F. and S.G.R. provided adjuvant GLA-SE for rhesus macaques immunization. S.S.A.-K., L.M., and M.C. contributed to clinical studies and neutralization epitope mapping.

Competing interests: B.F.H., H.-X.L., S.D., P.K.P., J.S., B.A., and Y.V. have filed International Patent Application PCT/US2014/034189 directed to the V3 glycopeptide, its synthesis, and its use as an immunogen. All other authors declare that they have no competing interests.

Data and materials availability: The GenBank accession numbers of V(D)J sequences for mAbs DH563, VRC41.01 and VRC41.02, and DH707 to DH710 are KY311872 to KY311873, KY308272 to KY308275, and KY311874 to KY311883, respectively.

Saunders[1,11], **Joseph Sodroski**[14], **Peter D. Kwong**[6], **John R. Mascola**[6], **Mattia Bonsignori**[1,2], **M. Anthony Moody**[1,5,15], **Samuel Danishefsky**[4], and **Barton F. Haynes**[1,2,5,*,†]

[1]Duke Human Vaccine Institute, Duke University School of Medicine, Durham, NC 27710, USA

[2]Department of Medicine, Duke University School of Medicine, Durham, NC 27710, USA

[3]Department of Pathology, Duke University School of Medicine, Durham, NC 27710, USA

[4]Department of Chemical Biology, Memorial Sloan Kettering Cancer Center, New York, NY 10065, USA

[5]Department of Immunology, Duke University School of Medicine, Durham, NC 27710, USA

[6]Vaccine Research Center, National Institute of Allergy and Infectious Diseases, National Institutes of Health, Bethesda, MD 20892, USA

[7]Infectious Disease Research Institute, Seattle, WA 98102, USA

[8]National Institute for Communicable Diseases, Johannesburg 2131, South Africa

[9]Center for the AIDS Programme of Research in South Africa, University of KwaZulu-Natal, Durban 4013, South Africa

[10]Department of Medicine, University of North Carolina at Chapel Hill, Chapel Hill, NC 27599, USA

[11]Department of Surgery, Duke University School of Medicine, Durham, NC 27710, USA

[12]Beth Israel Deaconess Medical Center, Boston, MA 02215, USA

[13]Department of Microbiology, Boston University School of Medicine, Boston, MA 02118, USA

[14]Dana-Farber Cancer Institute, Harvard Medical School, 450 Brookline Avenue, Boston, MA 02215, USA

[15]Department of Pediatrics, Duke University School of Medicine, Durham, NC 27710, USA

Abstract

A goal for an HIV-1 vaccine is to overcome virus variability by inducing broadly neutralizing antibodies (bnAbs). One key target of bnAbs is the glycan-polypeptide at the base of the envelope (Env) third variable loop (V3). We have designed and synthesized a homogeneous minimal immunogen with high-mannose glycans reflective of a native Env V3-glycan bnAb epitope (Man_9-V3). V3-glycan bnAbs bound to Man_9-V3 glycopeptide and native-like gp140 trimers with similar affinities. Fluorophore-labeled Man_9-V3 glycopeptides bound to bnAb memory B cells and were able to be used to isolate a V3-glycan bnAb from an HIV-1–infected individual. In rhesus macaques, immunization with Man_9-V3 induced V3-glycan-targeted antibodies. Thus, the Man_9-V3 glycopeptide closely mimics an HIV-1 V3-glycan bnAb epitope and can be used to isolate V3-glycan bnAbs.

INTRODUCTION

One strategy for the induction of HIV-1 glycan-directed broadly neutralizing antibodies (bnAbs) is to express trimeric forms of the envelope (Env) in structures that mimic the native trimer and bind to germ line–expressing naïve B cells (1). One problem for HIV-1 vaccine development has been the difficulty in design of such immunogens. Important criteria of Env nativeness are (i) that an HIV-1 antigen binds to bnAbs and (ii) that it can be used as a fluorophore-labeled protein for isolating bnAb-producing memory B cells by binding their B cell receptors (BCRs) (2–5) One such structural design recently reported is the BG505 SOSIP.664 Env trimer protein that presents a native-like Env conformation and is recognized by several classes of trimer-specific bnAbs (6–10). An alternative strategy for mimicking glycan bnAb epitopes is to produce immunogens that mimic HIV Env epitopes recognized by bnAb germline antibodies (11), while minimally presenting dominant strain-specific epitopes (12–15), either alone or in the context of heterologous protein scaffolds (16).

In studying the ontogeny of the V3-glycan bnAb DH270 lineage isolated from an African HIV-infected individual, we found that the un-mutated common ancestor (UCA) antibody for the DH270 lineage did not bind HIV-1 Env glycoprotein, either in solution or when expressed as a trimer on the cell surface (17). Here, we have synthesized a homogeneous and conformationally stable glycopeptide bearing two high-mannose undecasaccharides (Man_9) that binds to HIV-1 V3 bnAbs with affinities similar to that of the native-like BG505.664 SOSIP trimer. We have isolated members of a V3-glycan bnAb clonal lineage using either the synthetic fluorophore-labeled Man_9-V3 or SOSIP trimers, thus demonstrating that Man_9-V3 mimicked the HIV-1 V3-glycan bnAb epitope. Furthermore, the Man_9-V3 glycopeptide bound the UCA of the DH270 V3-glycan bnAb lineage (17) and induced V3-glycan–targeted antibodies in rhesus macaques.

RESULTS

Synthesis of Man_9-V3 glycopeptide

The crystal structure of the HIV-1 V3 bnAb PGT128 in complex with the gp120 Env outer domain containing a truncated V3 loop revealed the key antibody contacts with its glycosylated epitope (Fig. 1) (18). We synthesized a glycopeptide (Man_9-V3) that is based on the clade B JRFL HIV-1 isolate composed of the discontinuous epitope of PGT128 with deletion of residues 305 to 320, retention of P^{321}, and stabilization by a disulfide bridge between C^{296} and C^{331} (Fig. 1) (18). Man_9-V3 glycopeptide was chemically synthesized using a similar approach used to produce V1V2 glycopeptides (13). As controls, a biotinylated aglycone V3 peptide with no high-mannose glycans (Fig. 1) and a biotinylated Man_9 free glycan (Fig. 1 and Supplementary Materials, compound **9**) were also synthesized.

Antigenicity of Man_9-V3 glycopeptide

In biolayer interferometry (BLI) measurements, the V3-glycan bnAbs PGT128 and PGT125 bound specifically to Man_9-V3 glycopeptide but not to aglycone V3 peptide, as did the lectin concanavalin A (fig. S1A), which binds to both mannose and glucose. Monoclonal antibody (mAb) 2G12, which makes central contacts with the terminal mannose units at the

tip of the D1 arm of high-mannose glycans (19), also bound to Man_9-V3 glycopeptide but not to aglycone V3 peptide (fig. S1A). Each of the N^{332}-glycan–dependent bnAbs (PGT128 and PGT125) showed stronger binding to Man_9-V3 glycopeptide than to glycan only (Man_9) (fig. S1B), indicating that bnAb contacts with the V3 polypeptide in addition to Man_9 glycans (18). In enzyme-linked immunosorbent assay (ELISA), the half-maximal effective concentration (EC_{50}) of PGT128 (0.35 μg/ml) to Man_9-V3 was fivefold lower than that of PGT125 (1.75 μg/ml) (Fig. 2A). Apparent equilibrium dissociation constant (K_d) measurements by BLI of Man_9-V3 binding gave monovalent K_d values of 326 and 706 nM for PGT128 and PGT125, respectively (Fig. 2, B and C). However, binding of both V3 bnAbs was biphasic and strongly influenced by avidity effects, with PGT128-binding K_d being enhanced to 44 nM for the bivalent mode of binding (fig. S7A), indicating that the bivalent avidity effect could enhance the overall affinity by nearly an order of magnitude and likely mimicking the proposed cross-linking of viral Env spikes during PGT128 neutralization (18). Thus, the synthetic Man_9-V3 glycopeptide presented conformational epitopes required for glycan-dependent PGT128 and PGT125 bnAb binding. In addition, the high-mannose glycans presented on Man_9-V3 were appropriately spaced for the binding of the glycan-targeting bnAb 2G12 (fig. S1A).

Isolation of N^{332}-dependent clonal B cell lineage members

Plasma from the HIV-infected individual CH765 was predicted to have PGT128-like bnAb neutralization activity using a bnAb mapping analysis algorithm (20) (fig. S2A). CH765 plasma showed N^{332}-dependent neutralization activity (fig. S2B) and showed binding to Man_9-V3 but not to aglycone V3 (Fig. 3A). The SOSIP Env gp140 trimers present native-like Env conformations and BG505 SOSIP trimer as an affinity bait has been used to isolate quaternary bnAbs from blood memory B cells of an HIV-1–infected individual (3, 5, 10, 21). Therefore, using fluorophore-labeled native-like BG505 SOSIP trimers to bind to memory BCRs (10), we decorated memory B cells from donor CH765 with clade A BG505.T332N.SOSIP and clade C Env DU156.12.SOSIP gp140 trimer proteins. Dual SOSIP trimer–positive memory B cells were single cell–sorted, and immunoglobulin (Ig) heavy- and light-chain genes were amplified and recombinantly expressed (fig. S3A, table S1, and data set S3) (10). We isolated two antibodies, CH765-VRC41.01 and CH765-VRC41.02 (Fig. 3B). Similarly, mAb DH563 (Fig. 3B) was isolated after flow sorting of CH765 blood memory B cells decorated with fluorophore-labeled Man_9-V3 glycopeptide (fig. S3B, table S1, and data set S3). VRC41.01, VRC 41.02, and DH563 were clonally related (Fig. 3C); used V_H4–39 and V_κ4–69 heavy- and light-chain gene families, respectively; and had 20 to 21% V_H (variable region of immunoglobulin heavy chain) nucleotide mutations and a heavy-chain complementarity determining region 3 (HCDR3) length of 21 amino acids (table S1).

Specificity of VRC41.01, VRC41.02, and DH563 antibodies

Binding of the isolated antibodies to HIV-1 Env was N^{332}-dependent (fig. S4A), and site-directed mutagenesis of the BG505.W6M.C2 pseudovirus demonstrated VRC41.01 and VRC41.02 to be dependent on the N^{332} glycan for HIV-1 neutralization (fig. S4B). Further mapping on JRCSF.DB pseudovirus demonstrated VRC41.01 and VRC 41.02 to be sensitive to N^{301}A and N^{392}A mutations, but not to N^{295}A, N^{339}A, and T^{297}A mutations (fig. S4C).

Both PGT128 and VRC41.01 exhibited a similar phenotype, whereas PGT121 was sensitive only to the $N^{392}A$ mutation (fig. S4C). DH563, VRC41.01, and VRC41.02 mAbs reacted with Man_9-V3 glycopeptide but not with aglycone V3 peptide (fig. S5).

Like PGT128, positive autoreactivity in HEp-2 cell staining was observed for VRC41.01, whereas both VRC41.02 and DH563 did not react with HEp-2 cells (fig. S6). In a glycan array analysis, VRC41.01 gave a glycan binding profile that was similar to that of PGT128 by showing preferential binding to high-mannose glycans (Man_7, Man_8, and Man_9) (Fig. 3D). VRC41.01 also showed weaker responses to lower-order oligomannose glycans (Man_5 and Man_6) that did not bind to PGT128 (Fig. 3D). No detectable binding of the free glycans to either DH563 or VRC41.02 was observed (Fig. 3D).

Affinity of V3-glycan bnAb binding to Man_9-V3 glycopeptide and native-like SOSIP trimers

We compared affinities of the V3-glycan bnAbs VRC41.01, VRC41.02, and DH563 for Man_9-V3 glycopeptide and BG505 $T^{332}N$ SOSIP trimer (summarized in Fig. 3E). VRC41.01 bound to Man_9-V3 with an apparent K_d of 56 nM (Fig. 3E and fig. S7B), which was similar to the affinity values of PGT128 binding to Man_9-V3 (Fig. 3E and fig. S7A). Man_9-V3 affinities of both VRC41.02 (Fig. 3E and fig. S7C) and DH563 (Fig. 3E and fig. S7D) were weaker than that of VRC41.01 (K_d = 157 nM and K_d = 173 nM for VRC41.02 and DH563, respectively). As observed with Man_9-V3 glycopeptide, VRC41.01 bound to BG505. T332N. SOSIP gp140 with a K_d of 64.5 nM, which was similar to the affinity of PGT128 for the BG505 SOSIP (K_d = 41 nM) (Fig. 3E and fig. S8, A and B), whereas VRC41.02 bound with a weaker affinity of 166 nM (Fig. 3E and fig. S8C). However, DH563 bound to BG505 SOSIP trimer with higher affinity (K_d = 46 nM) (Fig. 3E and fig. S8D) than it did to Man_9-V3 glycopeptide (K_d = 173 nM) (Fig. 3E and fig. S7D). Thus, the affinities of the two VRC41 mAbs to BG505 SOSIP trimer were similar to their affinities for Man_9-V3 glycopeptide (Fig. 3E).

Neutralization breadth and potency of N^{332}-glycan–dependent mAbs

VRC41.01, VRC41.02, and DH563 V3-glycan bnAbs were tested for neutralization breadth and potency against 30 HIV pseudoviruses (Fig. 3F and table S2). VRC41.01 was the broadest and most potent of the DH563-VRC41 clones, neutralizing 63% of viruses with a median inhibitory concentration (IC_{50}) of 0.091 μg/ml. VRC41.01 was tested in a larger panel of 177 pseudoviruses and neutralized 56% of viruses with an IC_{50} of 0.620 μg/ml (fig. S9 and data set S2). Thus, using Man_9-V3 or native-like SOSIP trimers, we isolated from an HIV-infected individual three V3-glycan–specific bnAbs that belong to the same B cell clonal lineage.

Immunogenicity of Man_9-V3 glycopeptide in rhesus macaques

To test whether the synthetic Man_9-V3 glycoepeptide would induce antibodies that target the V3-glycan epitope, we immunized four rhesus macaques with monomeric Man_9-V3 glycopeptide formulated in the Toll-like receptor 4 agonist GLA-SE (glucopyranosyl lipid adjuvant–stable emulsion) adjuvant in a dose escalation study (50 to 500 μg of glycopeptide) (Fig. 4A). We detected plasma antibody binding in two of four macaques (#5994 and #5996) to both Man_9-V3 and aglycone V3 after the third 100-μg dose immunization. For macaque

#5994, higher titers of vaccine-induced responses were boosted with a higher-dose boost (500 μg) of Man_9-V3 glycopeptide (Fig. 4B). By flow sorting of Man_9-V3-AF647 and aglycone V3-BV421 decorated blood memory B cells from both animals (#5994 and #5996) harvested at either week 20 or week 52 after the final immunization, we isolated five mAbs that bound Man_9-V3 glycopeptide or aglycone V3 peptide constructs (figs. S10 and S11 and table S3). Four of the antibodies used V_H3 and one used V_H4 gene segments; V_H mutation frequencies ranged from 2% (DH707) to 11 to 12% (DH706, DH708, and DH710) (table S3). A variety of light chains were used, but all were V_λ(variable light chain λ) (table S3). Three antibodies (DH706, DH708, and DH710) selectively bound to Man_9-V3 glycopeptide, but not to aglycone V3, and two of them (DH706 and DH710) bound to CH848 transmitted founder (TF) gp120 and Consensus C (ConC) gp120 HIV-1 Envs (Fig. 4C and fig. S11). Deletion of the N-linked glycan at position N^{332} of the HIV-1 V3 loop resulted in decreased binding of DH706 and DH710 to the CH848 TF gp120 Env, compared to the wild type (Fig. 4C and fig. S11). DH706 and DH710 were tested for binding to JRFL and B.63521 Env glycoproteins grown either in the absence or in the presence of kifunensine, an endoplasmic reticulum mannosidase I inhibitor, to promote the density of N-linked high-mannose residues of the Env surface (22, 23). DH706 and DH710 preferentially bound Envs grown in the presence of kifunensine, suggesting that their binding to HIV-1 Env glycoproteins relied in part on high-mannose glycans (Fig. 4C). However, neither of these antibodies neutralized JRFL Env pseudoviruses when grown in the presence of kifunensine, indicating that the isolated mAbs are likely representative antibodies that lack sufficient HCDR3 length to bind to the V3-glycan site on virions with high affinity. A hallmark of V3-glycan bnAb UCAs is equal binding of Man_9-V3 glycopeptide and aglycone (17). mAb DH707 bound equally well to both aglycone and Man_9-V3 glycopeptide and had only 2% V_H mutations (fig. S11 and table S3). Thus, the Man_9-V3 glycopeptide induced antibody responses (for example, DH760 and DH710) in macaques targeted near the V3-glycan bnAb site.

DISCUSSION

Here, we show that the synthetic Man_9-V3 glycopeptide can be used to isolate V3-glycan bnAbs and can bind to mature V3-glycan bnAbs with similar affinities to native-like SOSIP trimers. That fluorophore-labeled Man_9-V3 glycopeptide can be recognized by V3-glycan bnAb memory BCRs attests to the ability of Man_9-V3 glycopeptide to mimic a V3-glycan HIV-1 Env bnAb epitope. In a companion study, the Man_9-V3 glycopeptide was successful in isolation of the most potent bnAb (DH270.6) of the DH270 V3-glycan lineage and also successfully used in isolation of the DH475 N^{332}-dependent cooperating B cell lineage antibody (17). Thus, the Man_9-V3 glycopeptide could be recognized not only by soluble bnAbs but also in the context of surface memory BCR expression.

The chemical synthesis process used for the production of the Man_9-V3 glycopeptide is distinct from the previously reported elegant synthesis of a full-length V3 glycopeptide that was synthesized using an endoglycosidase-catalyzed transglycosylation process to incorporate N-linked glycans (15). The Li *et al.* construct was designed to incorporate glycans at sites recognized by 2G12 (15, 24). Furthermore, Li *et al.* had pentasaccharides with Man_3 ($GlcNAc_2$-Man_3) at both positions (N^{295} and N^{332}) (15), whereas the glycopeptide described here had $GlcNAc_2$-Man_9 at both positions N^{301} and N^{332}. It is

notable that our V3 glycopeptide included the epitope sequences of the construct bound by PGT128 in its complex with the truncated outer domain eODmV3 (18). The apparent affinity (EC_{50}) by ELISA analysis of PGT128 IgG binding to eODmV3 was reported to be 46 nM (18), which is an order of magnitude weaker than PGT128 binding to Man_9-V3 (EC_{50} = 2.3 nM; Fig. 2A). Furthermore, the EC_{50} of PGT128 binding to cell surface trimer (2.8 nM) (18) is similar to the EC_{50} of its binding to the Man_9-V3 glycopeptide (2.3 nM; Fig. 2A). The antigenic elements of PGT128 epitope are therefore well preserved in our synthetic Man_9-V3 glycopeptide.

A major question has been what form of Env could initiate V3-glycan bnAb lineages. Neither soluble Env gp120 nor Env trimers bind V3-glycan bnAb soluble UCAs (17, 25). Bonsignori *et al.* have demonstrated that the Man_9-V3 glycopeptide and its aglycone form bind the UCA of the DH270 V3-glycan bnAb lineage (17). With affinity maturation in the DH270 bnAb, binding to the aglycone V3 diminished and binding to Man_9-V3 was increased (17). These observations raise the hypothesis that initiating immunogens for V3-glycan lineages may be denatured or Env fragments, which have been postulated to be the majority of Env present in infected cells (17, 26–28).

Our immunogenicity studies demonstrated that the monomeric V3 glycopeptide is not a potent immunogen, but rather could serve as a prime for subsequent boosts with Env immunogens that derive from evolved Envs from individuals that make V3-glycan bnAbs (17). Thus, as a monomer, the V3 glycopeptide primed precursors of V3-glycan B cell lineages to clonally expand. One induced antibody bound both the aglycone and the V3 glycopeptide, a trait of early precursors of V3-glycan bnAb lineages (17). Other isolated antibodies selectively bound only the Man_9-V3 glycopeptide and thus were dependent on binding to glycans at the V3 base. The next steps of the work are now multimerizing the V3 glycopeptide for higher-affinity BCR binding and then combining the Man_9-V3 glycopeptide prime with boosts of sequential Envs that, in an infected individual, induced bnAbs in HIV infection (17).

A limitation of this study is that immunizations were undertaken with the V3 glycopeptide monomer that did not have added T helper epitopes. We expect that multimerized V3 glycopeptide with added T helper epitopes will improve its immunogenicity. Second, the V3 glycopeptide only mimics PGT128-like V3-glycan bnAbs and does not mimic bnAbs that bind to complex glycans. Additional glycopeptides will be required to mimic other glycan-targeted bnAb sites. Nonetheless, the homogeneous Man_9-V3 glycopeptide mimics an HIV-1 Env V3-glycan bnAb epitope and can be used to define the memory B cell repertoire producing bnAbs, as well as to isolate V3-glycan bnAbs.

MATERIALS AND METHODS

Study design

The objective of the study was to design and synthesize a glycopeptide immunogen, bearing high-mannose glycans on two key asparagine residues (N332/N301), that mimics the epitope of a prevalent class of bnAbs that target the V3-glycan region of HIV-1 Env. An HIV-1–chronically infected donor (CH765) was recruited for plasma specimen based on V3-glycan

PGT128-like bnAb neutralization activity. Isolation of V3-glycan bnAbs was performed by labeling of both synthetic glycopeptide and SOSIP gp140 trimers with fluorophores and by flow cytometric sorting of antigen-specific memory B cells. Independent sorting with both SOSIP gp140 trimers and Man_9-V3 glycopeptide allowed the isolation from the CH765 donor plasma of three V3-glycan bnAbs that belong to the same lineage. Each isolated mAb was characterized by immunogenetics, glycan and Env binding, and neutralization breadth and potency analyses. Finally, the synthetic glycopeptide was used as an immunogen in rhesus macaques to test whether Man_9-V3 could induce antibodies that target the V3-glycan bnAb epitope. Five mAbs were isolated from blood memory B cells of immunized rhesus, and the mAbs were characterized for immunogenetics, glycan-dependent binding to Env proteins, and neutralization.

Human specimens

All work related to human subjects was in compliance with Institutional Review Board protocols approved by the Duke University Health System Institutional Review Board and the local ethics board at the site of enrollment. The participant in this study, an HIV-1–chronically infected donor (CH765, precise time of infection unknown), was recruited into the CHAVI 001 (Center for HIV/AIDS Vaccine Immunology 001) study, and blood obtained was processed to isolate peripheral blood mononuclear cells (PBMCs) that were stored in the vapor phase of liquid nitrogen tanks before their use in this study.

Synthesis of Man_9-V3 glycopeptide

A 30–amino acid V3 glycopeptide with oligomannose (Man_9-V3) glycans, based on the clade B JRFL mini-V3 construct (18), was chemically synthesized, as described earlier (13). A full description of the chemical synthesis is detailed in the Supplementary Text, and synthesis fragments are listed in bold reference to those fully described in the Supplementary Text. Briefly, linear trisaccharide glycosyl donor **S13** was synthesized with standard procedures and coupled to the core trisaccharide **S14** at C3 of the branching mannose residue under solvent-directing conditions. Subsequent removal of benzylidine furnished the desired glycosyl acceptor for the challenging regioslective [6+5] glycosylation at C6 of the aforementioned bridging mannose residue. Synthesis of branched pentasaccharide glycosyl donor **S12** was achieved with an efficient double mannosylation of a mannose thioglycoside **S23**. With these complex coupling partners in hand, glycosyl donor **S12** and acceptor **S29** were brought together with complete control of regioselectivity to furnish the desired fully protected $Man_9GlcNAc_2$ **S30**. Subsequent three-stage deprotection, purification, and Kochetkov anomeric amination furnished the desired β-glycosylamine **3** ready for installation on the peptide. Using our one-flask aspartylation/deprotection protocol (29), $Man_9GlcNAc_2$ glycosyl amine **3** was joined to the free carboxylic acid side chain at position 301 on fragment **4** and at position 332 on fragment **5**, followed by trifluoroacetic acid treatment to provide glycopeptide thioester **6** and N-terminal cysteinyl glycopeptide **7**. These two fragments were then joined by native chemical ligation, immediately followed by cyclization via disulfide formation to afford Man_9-V3-biotin. The control peptide, aglycone V3-biotin **2**, had an amino acid sequence identical to that of Man_9-V3-biotin **1**.

$Man_9GlcNAc_2$ (9) glycan synthesis

A full description of the chemical synthesis of **9** is detailed in the Supplementary Materials.

Briefly, $Man_9GlcNAc_2$–NH_2 **3** was treated with Biotin-OSu in dimethyl sulfoxide in the presence of 1-hydroxy-7-azabenzotriazole and *N,N*-diisopropylethylamine. After lyophilization, the product was purified by size exclusion chromatography to afford $Man_9GlcNAc_2$–NH–biotin **9**.

Production of SOSIP trimers

HIV-1 gp140 SOSIP-type molecules based on clade A strain BG505 (6, 8) and clade C strain DU156.12 (30) including the mutations ($A^{501}C$ and $T^{605}C$), the isoleucine-to-proline mutation at residue 559 ($I^{559}P$), the glycan site at residue 332 ($T^{332}N$), the mutation of the cleavage site to 6R (REKR to RRRRRR), and the truncation of the C terminus to residue 664 (all HIV-1 Env numbering according to the HX nomenclature) were used in this study. The BG505 SOSIP construct also encoded a C-terminal two–amino acid glycine-serine linker followed by an Avi-tag, whereas the DU156.12 construct encoded a C-terminal five–amino acid glycine-serine linker, a Thrombin cleavage site, a His6 purification tag, and a Strep-Tactin II purification tag followed by the Avi-tag sequence. The two HIV-1 SOSIP molecules were expressed as previously described (7) by cotransfecting with furin in human embryonic kidney 293F cells using 600 μg of HIV-1 SOSIP DNA and 150 μg of furin plasmid DNA. Transfection supernatants were harvested after 7 days, and the BG505 HIV-1 trimer supernatant was passed over either a 2G12 antibody– or VRC01 antibody–affinity column. After washing with phosphate-buffered saline (PBS), bound protein was eluted with 3 M $MgCl_2$ and 10 mM tris (pH 8.0). The eluate was concentrated to less than 4 ml with a Centricon-70 concentrator and applied to a 16/60 Superdex 200 column equilibrated in PBS. The DU156.12 HIV-1 trimer was purified by nickel and Strep-Tactin–affinity chromatography, followed by size exclusion chromatography using a Superdex 200 column equilibrated in PBS. In both cases, the peaks corresponding to trimeric HIV-1 Env were identified, pooled, concentrated, and either used immediately or flash-frozen in liquid nitrogen and stored at −80°C.

Antibody binding affinity measurements

Antibody binding to synthetic glycopeptide or to SOSIP gp140 trimers was measured by BLI (Pall ForteBio Octet RED96) analysis. The BLI assay was performed using streptavidin-coated sensors (Pall ForteBio) to capture either biotin-tagged Man_9-V3 glycopeptide or aglycone V3 peptide. The V3 peptide–immobilized sensors were dipped into varying concentrations of antibodies after blocking of sensors in 0.1% bovine serum albumin (BSA). Antibody concentrations ranged from 0.5 to 150 μg/ml, and nonspecific binding interactions were subtracted using the control anti–respiratory syncytial virus mAb palivizumab (Synagis). Rate constants and apparent K_d were calculated by global curve fitting analyses to the bivalent avidity model of binding responses with a 10- to 15-min association and 15-min dissociation interaction time. The apparent K_d values for monovalent interactions of the antibodies were estimated using the faster components of the association and dissociation rates k_{a1} and k_{d1}, respectively. For binding to Man_9-V3 glycopeptide or BG505 SOSIP gp140 where avidity effects were strong and binding curves could not be

resolved into their components, apparent K_d values were derived using dose-response curves at varying antibody concentrations (0.5 to 80 μg/ml) and using a nonlinear four-paramater curve fitting analysis.

Isolation of DH563 mAb

Biotinylated Man_9-V3 peptides were tetramerized via streptavidin and conjugated with either AF647 (Thermo Scientific) or BV421 (BioLegend) dyes. Peptide tetramer quality after conjugation was assessed by flow cytometry to a panel of well-characterized HIV-1 V3-glycan antibodies (PGT128 and 2G12) and linear V3 antibodies (F39F) attached to polymer beads. PBMCs from donor CH765 were stained with LIVE/DEAD Fixable Aqua Stain (Thermo Scientific), anti-human IgM [fluorescein isothiocyanate (FITC)], CD3 (PE-Cy5), CD235a (PE-Cy5), CD19 (APC-Cy7), and CD27 (PE-Cy7) (BD Biosciences); anti-human antibodies against IgD (PE); anti-human antibodies against CD10 [ECD (R-Phycoerythrim–Texas Red-X], CD38 (APC-AF700), CD19 (APC-Cy7), CD16 (BV570), and CD14 (BV605) (BioLegend); and $Man_9GlcNac_2$ V3 tetramer in both AF647 and BV421. PBMCs that were Aqua Stain$^-$, CD14$^-$, CD16$^-$, CD3$^-$, CD235a$^-$, IgD$^-$, positive for CD19$^+$, and negative for surface IgD were defined as memory B cells; these cells were then gated for Man_9-V3$^+$ positivity in both AF647 and BV421 and were single cell–sorted using a BD FACSAria II into 96-well plates containing 20 μl of reverse transcriptase (RT) buffer. Complementary DNA (cDNA) synthesis was performed, as previously described (31). Ig heavy (V_H) chains were polymerase chain reaction (PCR)–amplified using a nested approach. V_H genes were amplified in the first round of amplification from (4), followed by nested amplification of V_H, V_κ (variable light chain κ), and V_λ genes as performed in (32). Primers used are listed in data set S3. PCR products were analyzed on 2% SYBR Safe E-Gels (Invitrogen). PCR-amplified V_H and V_L genes were purified and sequenced. Sequences were analyzed, and V(D)J arrangements were inferred using computational methods, as previously described (33, 34).

Isolation of VRC41.01 and VRC41.02 mAbs

Biotinylated BG505.T332N.SOSIP and DU156.12.SOSIP trimers were tetramerized via streptavidin-linked PE and APC (Invitrogen), respectively, as previously described (5, 35). Peptide tetramer quality after conjugation was assessed by flow cytometry to a panel of well-characterized HIV-1–specific bnAbs. PBMCs from donor CH765 were stained with LIVE/DEAD fixable violet dead cell dye (Invitrogen), anti-human IgG (FITC), anti-human CD19 (Cy7-PE), anti-human CD3 (Cy7-APC), anti-human CD8 (BV711), anti-human CD14 (BV605), BG505.T332N.SOSIP trimer (PE), and DU156.12.SOSIP trimer (APC). PBMCs that were violet dye$^-$, CD3$^-$, CD8$^-$, CD14$^-$, CD19$^+$, IgG$^+$, and BG505.T332N.SOSIP$^+$ and/or DU156.12.SOSIP$^+$ were single cell–sorted using a BD FACSAria II into 96-well plates containing 20 μl of RT buffer, and cDNA synthesis was performed, as previously described (20). Ig heavy (V_H) and light (V_L) chains were PCR-amplified using a nested approach. First- and second-round amplification of V_H, V_κ, and V_λ genes was carried out as in (20), with primers grouped as previously described (35). PCR products were analyzed on 1% 96-well ethidium bromide–stained precast gels (Embi Tec). PCR-amplified V_H and V_L genes were purified and sequenced. Sequences were analyzed, and V(D)J arrangements were inferred using IMGT/V-Quest (www.imgt.org).

Transient and recombinant antibody expression

Transient and recombinant mAb production was performed, as previously described, for DH563 (32, 36). VRC41.01 and VRC41.02 were produced, as previously described (20).

Enzyme-linked immunosorbent assay

Screening of recombinant mAbs sorted with fluorophore-conjugated Man_9-V3 was performed, as previously described (36). Transient transfected antibodies as well as purified DH563 were assessed for binding to heterologous Env (ConC gp120, VRCb gp120, and ConS gp140). N^{332} sensitivity was assessed by reduction in binding to N^{332}A mutant Env compared to wild-type Env. Binding to Man_9-V3-biotin and aglycone V3-biotin was determined as follows. Briefly, streptavidin (2 μg/ml) in coating buffer (0.1 M $NaHCO_3$, pH 9.6) was used to coat 384-well high-binding ELISA plates at 15 μl per well at 4°C overnight. Plates were washed with PBS + 0.05% Tween 20 and blocked with 3% BSA in PBS at room temperature for 1 hour. The blocked plates were washed and 10 μl of biotinylated Man_9-V3 and biotinylated aglycone V3 was diluted to 1 μg/ml in 1% BSA in PBS + 0.05% Tween 20 at room temperature for 1 hour. Plates were again washed, and serial threefold dilutions of purified mAbs ranging from 0 to 100 μg/ml in 1% BSA in PBS + 0.05% Tween 20 were added and incubated at room temperature for 1 hour. After incubation, plates were washed twice and incubated with horseradish peroxidase (HRP) goat anti-human IgG (1:10,000) diluted in 1% BSA in PBS + 0.05% Tween 20 at room temperature for 1 hour. These plates were washed four times with and developed with tetramethyl benzidine substrate (20 μl per well) (SureBlue Reserve) for 15 min. The HRP reaction was stopped with 1 M HCl (20 μl per well), and OD (at 450 nm) was determined. The EC_{50} of mAbs to HIV-1 Env, Man_9-V3, and aglycone V3 was determined and expressed as the concentration of mAb.

Antibody reactivity by indirect immunofluorescence

Indirect immunofluorescence binding of recombinant mAbs to HEp-2 cells (Inverness Medical Professional Diagnostics) was performed as follows. On a predetermined spot on an antinuclear antibody HEp-2 kit slide, 20 μl of antibody at 50 μg/ml was incubated for 25 min at room temperature, washed, and developed for 25 min with 20 μl of goat anti-human Ig-FITC at 20 μg/ml (SouthernBiotech). All incubations were performed in humidified chambers in the dark. Before fixation, slides were washed and dried, and a drop of 33% glycerol was placed on each spot. Images were taken on an Olympus AX70 with SpotFlex FX1520 charge-coupled device with a UPlanFl 40× (numerical aperture, 0.75) objective at 25°C in the FITC channel using SPOT software. All images were acquired for the time specified in the figure legend. Image layout and scaling were performed in Adobe Photoshop without image manipulation.

Neutralization assays

Antibody neutralizing activity was assessed via a TZM-bl cell-based neutralization assay (37). Neutralization breadth and potency for DH563/VRC41 family of V3-glycan antibodies were tested in a multi-clade panel of 30 tier 2 Env pseudoviruses. Neutralization breadth and potency of VRC41.01 against a panel of 177 geographically and genetically diverse Env

pseudoviruses representing the major subtypes and circulating recombinant forms were performed, as previously described (5, 20).

Oligomannose glycan array immunostaining

Custom glycan arrays printed in a 24-subarray format were purchased from Z Biotech. The natural source glycans $GlcNAc_2$, $Man_5GlcNAc_2$, $Man_6GlcNAc_2$, $Man_7GlcNAc_2$ D1, $Man_7GlcNAc_2$ D3, $Man_8GlcNAc_2$ D1D3, and $Man_9GlcNAc_2$ were printed onto the array using hydrazide chemistry. Within each subarray, the glycans were printed in triplicate at 100, 33, and 10 μM concentrations, and print buffer alone was printed as a background binding control. Human IgG was printed within each subarray to serve as a detection control. For immunostaining of each subarray, the arrays were placed in an ArraySlide-24 holder (Gel Company). Each subarray was hydrated in Milli-Q (Millipore) water for 2 min. Hydrazide Glycan Blocking Buffer (Z Biotech) was used to block each subarray for 1 hour. The subarrays were sealed with adhesive foil and were shaken at 40 rpm during all incubation steps. The blocking buffer was aspirated, and antibody (50 μg/ml) diluted in Glycan Array Assay Buffer (Z Biotech) was incubated on an individual subarray for 1 hour. As a positive control, biotinylated concanavalin A (20 μg/ml) was assayed in parallel on each array. The array was washed five times with PBS + 0.05% Tween 20. Antibody binding to glycan was detected with a Cy3-conjugated anti-human IgG antibody (Sigma). Biotinylated concanavalin A binding was detected with Cy3-conjugated streptavidin (Sigma). The array was washed five times with PBS + 0.05% Tween 20 and one time with 0.01 × PBS and spun dry. The fluorescence of each feature was read with a GenePix 4000B instrument (Molecular Devices) and quantified using GenePix software (version 7, Molecular Devices). Any fluorescence observed in the print buffer alone was subtracted from the mean fluorescence for each glycan.

Immunizations

Immunization of rhesus macaques and blood draws were performed at Bioqual Inc. according to the schedule in Fig. 4. Indian origin rhesus macaques were immunized intramuscularly with 50, 100, or 500 μg of Man_9-V3 monomeric glycopeptide formulated in GLA-SE adjuvant, and blood samples were collected 2 weeks after immunization. All rhesus macaques were maintained in accordance with the Association for Assessment and Accreditation of Laboratory Animals. Research was conducted in compliance with the Animal Welfare Act and other federal statutes and regulations relating to animals and experiments involving animals and adheres to principles stated in the *Guide for the Care and Use of Laboratory Animals* (NRC Publication, 2011 edition).

Isolation of DH706-DH710 rhesus mAbs

Man_9-V3 and/or aglycone V3–specific memory B cells from macaques #5994 and #5996 were sorted by flow cytometry, as previously described (38). Briefly, 1×10^7 PBMCs were decorated with a B cell antibody panel that cross-reacts with rhesus B cells [CD14 (BV570), CD3 (peridinin chlorophyll protein–Cy5.5), CD20 (FITC), CD27 (APC-Cy7), and IgD (PE) (BD Biosciences)], AF647-tagged Man_9-V3, and BV421-tagged aglycone V3. Antigen-specific memory B cells were gated as $D3^-CD14^-CD20^+CD27^+sIgD^-$, and antibodies were sorted [on the basis of the reactivities Man_9-$V3^+$, aglycone $V3^-$ (DH706, DH708, and

DH710), Man_9-$V3^+$, aglycone $V3^+$ (DH707), and Man_9-$V3^-$, aglycone $V3^+$ (DH709)] into 96-well PCR plates containing 20 μl of reverse transcription reaction buffer that included 5 μl of 5× first-strand cDNA buffer, 1.25 μl of dithiothreitol, 0.5 μl of RNaseOUT (Life Technologies), 0.0625 μl of Igepal (Sigma-Aldrich), and 13.25 μl of ultrapure deionized water (Life Technologies). Rhesus macaque V_HDJ_H and V_LJ_L segments were isolated by single-cell reverse transcription–PCR using methods previously described (39). Isolated V(D)J gene fragments were used for the construction of linear expression cassettes for production of recombinant mAbs in 293T cells (39).

Production of kifunensine-treated HIV-1 Envs

One milligram of plasmid Env DNA per liter of cells was diluted in DulbeccosmodifiedEaglesmediumandmixedwithPEI(polyethylenimine). PEI:DNA mixtures were added to cells for 4 hours. 293F (Invitrogen) cells were subsequently washed and diluted to 1.25 million cells/ml in FreeStyle 293 medium (Invitrogen). In instances where high-mannose glycosylation was desired, kifunensine (Sigma-Aldrich) was dissolved in PBS and added once to the cell culture medium to a final concentration of 25 μM. The cells were cultured for 5 days, and on the fifth day, the cell culture medium was cleared of cells by centrifugation and filtered with a 0.8-μm filter. The cell culture was concentrated with a Vivaflow 50 (Sartorius) with a molecular mass cutoff of 10 kDa. The concentrated cell culture supernatant was rotated with lectin beads (Vistar Labs) overnight at 4°C. The beads were pelleted by centrifugation the next day and resuspended in MES wash buffer. The lectin beads were washed twice, and the protein was eluted with methyl-α-pyranoside. The protein was buffer-exchanged into PBS and stored at −80°C.

Supplementary Material

Refer to Web version on PubMed Central for supplementary material.

Acknowledgments

We thank D. Marshall, J. Whitesides, E. Friberg, E. Dunford, the Duke Human Vaccine Institute Flow Cytometry Core, and N. Tumba (National Institute for Communicable Diseases, South Africa) for technical assistance.

Funding: This study was supported by UM-1 AI100645 from NIH, National Institute of Allergy and Infectious Diseases (NIAID), Division of AIDS CHAVI–Immunogen Discovery grant, R01 AI120801-01 (K.O.S.), Medical Scientist Training Program training grant T32GM007171 (R.R.M.), Ruth L. Kirschstein National Research Service Award F30-AI122982-0, NIAID (R.R.M.), and the intramural research program of the Vaccine Research Center, NIAID.

REFERENCES AND NOTES

1. Mascola JR, Haynes BF. HIV-1 neutralizing antibodies: Understanding nature’s pathways. Immunol Rev. 2013; 254:225–244. [PubMed: 23772623]
2. Scheid JF, Mouquet H, Feldhahn N, Seaman MS, Velinzon K, Pietzsch J, Ott RG, Anthony RM, Zebroski H, Hurley A, Phogat A, Chakrabarti B, Li Y, Connors M, Pereyra F, Walker BD, Wardemann H, Ho D, Wyatt RT, Mascola JR, Ravetch JV, Nussenzweig MC. Broad diversity of neutralizing antibodies isolated from memory B cells in HIV-infected individuals. Nature. 2009; 458:636–640. [PubMed: 19287373]

3. Scheid JF, Mouquet H, Feldhahn N, Walker BD, Pereyra F, Cutrell E, Seaman MS, Mascola JR, Wyatt RT, Wardemann H, Nussenzweig MC. A method for identification of HIV gp140 binding memory B cells in human blood. J Immunol Methods. 2009; 343:65–67. [PubMed: 19100741]

4. Scheid JF, Mouquet H, Ueberheide B, Diskin R, Klein F, Oliveira TYK, Pietzsch J, Fenyo D, Abadir A, Velinzon K, Hurley A, Myung S, Boulad F, Poignard P, Burton DR, Pereyra F, Ho DD, Walker BD, Seaman MS, Bjorkman PJ, Chait BT, Nussenzweig MC. Sequence and structural convergence of broad and potent HIV antibodies that mimic CD4 binding. Science. 2011; 333:1633–1637. [PubMed: 21764753]

5. Wu X, Yang Z-Y, Li Y, Hogerkorp C-M, Schief WR, Seaman MS, Zhou T, Schmidt SD, Wu L, Xu L, Longo NS, McKee K, O'Dell S, Louder MK, Wycuff DL, Feng Y, Nason M, Doria-Rose N, Connors M, Kwong PD, Roederer M, Wyatt RT, Nabel GJ, Mascola JR. Rational design of envelope identifies broadly neutralizing human monoclonal antibodies to HIV-1. Science. 2010; 329:856–861. [PubMed: 20616233]

6. Julien J-P, Cupo A, Sok D, Stanfield RL, Lyumkis D, Deller MC, Klasse P-J, Burton DR, Sanders RW, Moore JP, Ward AB, Wilson IA. Crystal structure of a soluble cleaved HIV-1 envelope trimer. Science. 2013; 342:1477–1483. [PubMed: 24179159]

7. Pancera M, Zhou T, Druz A, Georgiev IS, Soto C, Gorman J, Huang J, Acharya P, Chuang G-Y, Ofek G, Stewart-Jones GB, Stuckey J, Bailer RT, Joyce MG, Louder MK, Tumba N, Yang Y, Zhang B, Cohen MS, Haynes BF, Mascola JR, Morris L, Munro JB, Blanchard SC, Mothes W, Connors M, Kwong PD. Structure and immune recognition of trimeric prefusion HIV-1 Env. Nature. 2014; 514:455–461. [PubMed: 25296255]

8. Sanders RW, Derking R, Cupo A, Julien J-P, Yasmeen A, de Val N, Kim HJ, Blattner C, de la Peña AT, Korzun J, Golabek M, de Los Reyes K, Ketas TJ, van Gils MJ, King CR, Wilson IA, Ward AB, Klasse PJ, Moore JP. A next-generation cleaved, soluble HIV-1 Env trimer, BG505 SOSIP.664 gp140, expresses multiple epitopes for broadly neutralizing but not non-neutralizing antibodies. PLOS Pathog. 2013; 9:e1003618. [PubMed: 24068931]

9. Sanders RW, van Gils MJ, Derking R, Sok D, Ketas TJ, Burger JA, Ozorowski G, Cupo A, Simonich C, Goo L, Arendt H, Kim HJ, Lee JH, Pugach P, Williams M, Debnath G, Moldt B, van Breemen MJ, Isik G, Medina-Ramírez M, Back JW, Koff WC, Julien J-P, Rakasz EG, Seaman MS, Guttman M, Lee KK, Klasse PJ, LaBranche C, Schief WR, Wilson IA, Overbaugh J, Burton DR, Ward AB, Montefiori DC, Dean H, Moore JP. HIV-1 VACCINES. HIV-1 neutralizing antibodies induced by native-like envelope trimers. Science. 2015; 349:aac4223. [PubMed: 26089353]

10. Sok D, van Gils MJ, Pauthner M, Julien J-P, Saye-Francisco KL, Hsueh J, Briney B, Lee JH, Le KM, Lee PS, Hua Y, Seaman MS, Moore JP, Ward AB, Wilson IA, Sanders RW, Burton DR. Recombinant HIV envelope trimer selects for quaternary-dependent antibodies targeting the trimer apex. Proc Natl Acad Sci USA. 2014; 111:17624–17629. [PubMed: 25422458]

11. Haynes BF, Kelsoe G, Harrison SC, Kepler TB. B-cell–lineage immunogen design in vaccine development with HIV-1 as a case study. Nat Biotechnol. 2012; 30:423–433. [PubMed: 22565972]

12. Alam SM, Dennison SM, Aussedat B, Vohra Y, Park PK, Fernández-Tejada A, Stewart S, Jaeger FH, Anasti K, Blinn JH, Kepler TB, Bonsignori M, Liao H-X, Sodroski JG, Danishefsky SJ, Haynes BF. Recognition of synthetic glycopeptides by HIV-1 broadly neutralizing antibodies and their unmutated ancestors. Proc Natl Acad Sci USA. 2013; 110:18214–18219. [PubMed: 24145434]

13. Aussedat B, Vohra Y, Park PK, Fernández-Tejada A, Alam SM, Dennison SM, Jaeger FH, Anasti K, Stewart S, Blinn JH, Liao H-X, Sodroski JG, Haynes BF, Danishefsky SJ. Chemical synthesis of highly congested gp120 V1V2 *N*-glycopeptide antigens for potential HIV-1-directed vaccines. J Am Chem Soc. 2013; 135:13113–13120. [PubMed: 23915436]

14. Fernández-Tejada A, Haynes BF, Danishefsky SJ. Designing synthetic vaccines for HIV. Expert Rev Vaccines. 2015; 14:815–831. [PubMed: 25824661]

15. Li H, Li B, Song H, Breydo L, Baskakov IV, Wang L-X. Chemoenzymatic synthesis of HIV-1 V3 glycopeptides carrying two *N*-glycans and effects of glycosylation on the peptide domain. J Org Chem. 2005; 70:9990–9996. [PubMed: 16292832]

16. Zhou T, Zhu J, Yang Y, Gorman J, Ofek G, Srivatsan S, Druz A, Lees CR, Lu G, Soto C, Stuckey J, Burton DR, Koff WC, Connors M, Kwong PD. Transplanting supersites of HIV-1 vulnerability. PLOS ONE. 2014; 9:e99881. [PubMed: 24992528]

17. Bonsignori M, Kreider EF, Fera D, Meyerhoff RR, Bradley T, Wiehe K, Alam SM, Aussedat B, Walkowicz WE, Hwang KK, Saunders KO, Zhang R, Gladden MA, Monroe A, Kumar A, SMX, Cooper M, Louder MK, McKee K, Bailer RT, Pier BW, Jette CA, Kelsoe G, Williams WB, Morris L, Kappes J, Wagh K, Kamanga G, Cohen MS, Hraber PT, Montefiori DC, Trama A, Liao HX, Kepler TB, Moody MA, Gao F, Danishefsky SJ, Mascola JR, Shaw GM, Hahn BH, Harrison SC, Korber BT, Haynes BF. Staged induction of HIV-1 glycan-dependent broadly neutralizing antibodies. Sci Transl Med. 2017; 9:eaai7514. [PubMed: 28298420]

18. Pejchal R, Doores KJ, Walker LM, Khayat R, Huang P-S, Wang S-K, Stanfield RL, Julien J-P, Ramos A, Crispin M, Depetris R, Katpally U, Marozsan A, Cupo A, Maloveste S, Liu Y, McBride R, Ito Y, Sanders RW, Ogohara C, Paulson JC, Feizi T, Scanlan CN, Wong C-H, Moore JP, Olson WC, Ward AB, Poignard P, Schief WR, Burton DR, Wilson IA. A potent and broad neutralizing antibody recognizes and penetrates the HIV glycan shield. Science. 2011; 334:1097–1103. [PubMed: 21998254]

19. Calarese DA, Scanlan CN, Zwick MB, Deechongkit S, Mimura Y, Kunert R, Zhu P, Wormald MR, Stanfield RL, Roux KH, Kelly JW, Rudd PM, Dwek RA, Katinger H, Burton DR, Wilson IA. Antibody domain exchange is an immunological solution to carbohydrate cluster recognition. Science. 2003; 300:2065–2071. [PubMed: 12829775]

20. Georgiev IS, Doria-Rose NA, Zhou T, Kwon YD, Staupe RP, Moquin S, Chuang G-Y, Louder MK, Schmidt SD, Altae-Tran HR, Bailer RT, McKee K, Nason M, O'Dell S, Ofek G, Pancera M, Srivatsan S, Shapiro L, Connors M, Migueles SA, Morris L, Nishimura Y, Martin MA, Mascola JR, Kwong PD. Delineating antibody recognition in polyclonal sera from patterns of HIV-1 isolate neutralization. Science. 2013; 340:751–756. [PubMed: 23661761]

21. Liao H-X, Bonsignori M, Alam SM, McLellan JS, Tomaras GD, Moody MA, Kozink DM, Hwang K-K, Chen X, Tsao C-Y, Liu P, Lu X, Parks RJ, Montefiori DC, Ferrari G, Pollara J, Rao M, Peachman KK, Santra S, Letvin NL, Karasavvas N, Yang Z-Y, Dai K, Pancera M, Gorman J, Wiehe K, Nicely NI, Rerks-Ngarm S, Nitayaphan S, Kaewkungwal J, Pitisuttithum P, Tartaglia J, Sinangil F, Kim JH, Michael NL, Kepler TB, Kwong PD, Mascola JR, Nabel GJ, Pinter A, Zolla-Pazner S, Haynes BF. Vaccine induction of antibodies against a structurally heterogeneous site of immune pressure within HIV-1 envelope protein variable regions 1 and 2. Immunity. 2013; 38:176–186. [PubMed: 23313589]

22. Doores KJ, Burton DR. Variable loop glycan dependency of the broad and potent HIV-1-neutralizing antibodies PG9 and PG16. J Virol. 2010; 84:10510–10521. [PubMed: 20686044]

23. Scanlan CN, Ritchie GE, Baruah K, Crispin M, Harvey DJ, Singer BB, Lucka L, Wormald MR, Wentworth P Jr, Zitzmann N, Rudd PM, Burton DR, Dwek RA. Inhibition of mammalian glycan biosynthesis produces non-self antigens for a broadly neutralising, HIV-1 specific antibody. J Mol Biol. 2007; 372:16–22. [PubMed: 17631311]

24. Scanlan CN, Pantophlet R, Wormald MR, Ollman Saphire E, Stanfield R, Wilson IA, Katinger H, Dwek RA, Rudd PM, Burton DR. The broadly neutralizing anti-human immunodeficiency virus type 1 antibody 2G12 recognizes a cluster of α 1→2 mannose residues on the outer face of gp120. J Virol. 2002; 76:7306–7321. [PubMed: 12072529]

25. Sok D, Laserson U, Laserson J, Liu Y, Vigneault F, Julien J-P, Briney B, Ramos A, Saye KF, Le K, Mahan A, Wang S, Kardar M, Yaari G, Walker LM, Simen BB, St John EP, Chan-Hui P-Y, Swiderek K, Kleinstein SH, Alter G, Seaman MS, Chakraborty AK, Koller D, Wilson IA, Church GM, Burton DR, Poignard P. The effects of somatic hypermutation on neutralization and binding in the PGT121 family of broadly neutralizing HIV antibodies. PLOS Pathog. 2013; 9:e1003754. [PubMed: 24278016]

26. Hangartner L, Zinkernagel RM, Hengartner H. Antiviral antibody responses: The two extremes of a wide spectrum. Nat Rev Immunol. 2006; 6:231–243. [PubMed: 16498452]

27. Kuraoka M, Schmidt AG, Nojima T, Feng F, Watanabe A, Kitamura D, Harrison SC, Kepler TB, Kelsoe G. Complex antigens drive permissive clonal selection in germinal centers. Immunity. 2016; 44:542–552. [PubMed: 26948373]

28. Crooks ET, Tong T, Osawa K, Binley JM. Enzyme digests eliminate nonfunctional Env from HIV-1 particle surfaces, leaving native Env trimers intact and viral infectivity unaffected. J Virol. 2011; 85:5825–5839. [PubMed: 21471242]

29. Wang P, Aussedat B, Vohra Y, Danishefsky SJ. An advance in the chemical synthesis of homogeneous N-linked glycopeptide by convergent aspartylation. Angew Chem Int Ed Engl. 2012; 51:11571–11575. [PubMed: 23011954]
30. Li M, Salazar-Gonzalez JF, Derdeyn CA, Morris L, Williamson C, Robinson JE, Decker JM, Li Y, Salazar MG, Polonis VR, Mlisana K, Karim SA, Hong K, Greene KM, Bilska M, Zhou J, Allen S, Chomba E, Mulenga J, Vwalika C, Gao F, Zhang M, Korber BTM, Hunter E, Hahn BH, Montefiori DC. Genetic and neutralization properties of subtype C human immunodeficiency virus type 1 molecular *env* clones from acute and early heterosexually acquired infections in Southern Africa. J Virol. 2006; 80:11776–11790. [PubMed: 16971434]
31. Wardemann H, Yurasov S, Schaefer A, Young JW, Meffre E, Nussenzweig MC. Predominant autoantibody production by early human B cell precursors. Science. 2003; 301:1374–1377. [PubMed: 12920303]
32. Liao H-X, Levesque MC, Nagel A, Dixon A, Zhang R, Walter E, Parks R, Whitesides J, Marshall DJ, Hwang K-K, Yang Y, Chen X, Gao F, Munshaw S, Kepler TB, Denny T, Moody MA, Haynes BF. High-throughput isolation of immunoglobulin genes from single human B cells and expression as monoclonal antibodies. J Virol Methods. 2009; 158:171–179. [PubMed: 19428587]
33. Kepler TB. Reconstructing a B-cell clonal lineage. I. Statistical inference of unobserved ancestors. F1000Res. 2013; 2:103. [PubMed: 24555054]
34. Kepler TB, Munshaw S, Wiehe K, Zhang R, Yu J-S, Woods CW, Denny TN, Tomaras GD, Alam SM, Moody MA, Kelsoe G, Liao H-X, Haynes BF. Reconstructing a B-cell clonal lineage. II. Mutation, selection, and affinity maturation. Front Immunol. 2014; 5:170. [PubMed: 24795717]
35. Doria-Rose NA, Bhiman JN, Roark RS, Schramm CA, Gorman J, Chuang G-Y, Pancera M, Cale EM, Ernandes MJ, Louder MK, Asokan M, Bailer RT, Druz A, Fraschilla IR, Garrett NJ, Jarosinski M, Lynch RM, McKee K, O'Dell S, Pegu A, Schmidt SD, Staupe RP, Sutton MS, Wang K, Wibmer CK, Haynes BF, Abdool-Karim S, Shapiro L, Kwong PD, Moore PL, Morris L, Mascola JR. New member of the V1V2-directed CAP256-VRC26 lineage that shows increased breadth and exceptional potency. J Virol. 2015; 90:76–91. [PubMed: 26468542]
36. Liao H-X, Chen X, Munshaw S, Zhang R, Marshall DJ, Vandergrift N, Whitesides JF, Lu X, Yu JS, Hwang K-K, Gao F, Markowitz M, Heath SL, Bar KJ, Goepfert PA, Montefiori DC, Shaw GC, Alam SM, Margolis DM, Denny TN, Boyd SD, Marshal E, Egholm M, Simen BB, Hanczaruk B, Fire AZ, Voss G, Kelsoe G, Tomaras GD, Moody MA, Kepler TB, Haynes BF. Initial antibodies binding to HIV-1 gp41 in acutely infected subjects are polyreactive and highly mutated. J Exp Med. 2011; 208:2237–2249. [PubMed: 21987658]
37. Sarzotti-Kelsoe M, Bailer RT, Turk E, Lin C-l, Bilska M, Greene KM, Gao H, Todd CA, Ozaki DA, Seaman MS, Mascola JR, Montefiori DC. Optimization and validation of the TZM-bl assay for standardized assessments of neutralizing antibodies against HIV-1. J Immunol Methods. 2014; 409:131–146. [PubMed: 24291345]
38. Morris L, Chen X, Alam M, Tomaras G, Zhang R, Marshall DJ, Chen B, Parks R, Foulger A, Jaeger F, Donathan M, Bilska M, Gray ES, Abdool Karim SS, Kepler TB, Whitesides J, Montefiori D, Moody MA, Liao H-X, Haynes BF. Isolation of a human anti-HIV gp41 membrane proximal region neutralizing antibody by antigen-specific single B cell sorting. PLOS ONE. 2011; 6:e23532. [PubMed: 21980336]
39. Wiehe K, Easterhoff D, Luo K, Nicely NI, Bradley T, Jaeger FH, Dennison SM, Zhang R, Lloyd KE, Stolarchuk C, Parks R, Sutherland LL, Scearce RM, Morris L, Kaewkungwal J, Nitayaphan S, Pitisuttithum P, Rerks-Ngarm S, Sinangil F, Phogat S, Michael NL, Kim JH, Kelsoe G, Montefiori DC, Tomaras GD, Bonsignori M, Santra S, Kepler TB, Alam SM, Moody MA, Liao H-X, Haynes BF. Antibody light-chain-restricted recognition of the site of immune pressure in the RV144 HIV-1 vaccine trial is phylogenetically conserved. Immunity. 2014; 41:909–918. [PubMed: 25526306]
40. Chayajarus K, Chambers DJ, Chughtai MJ, Fairbanks AJ. Stereospecific synthesis of 1,2-*cis* glycosides by vinyl-mediated IAD. Org Lett. 2004; 6:3797–3800. [PubMed: 15469352]
41. Crich D, Li H, Yao Q, Wink DJ, Sommer RD, Rheingold AL. Direct synthesis of β-mannans. A hexameric [→3)-β-D-Man-(1→4)-β-D-Man-(1]$_3$ subunit of the antigenic polysaccharides from *Leptospira biflexa* and the octameric (1→2)-linked β-D-Mannan of the *Candida albicans* phospholipomannan. X-ray crystal structure of a protected tetramer. J Am Chem Soc. 2001; 123:5826–5828. [PubMed: 11403627]

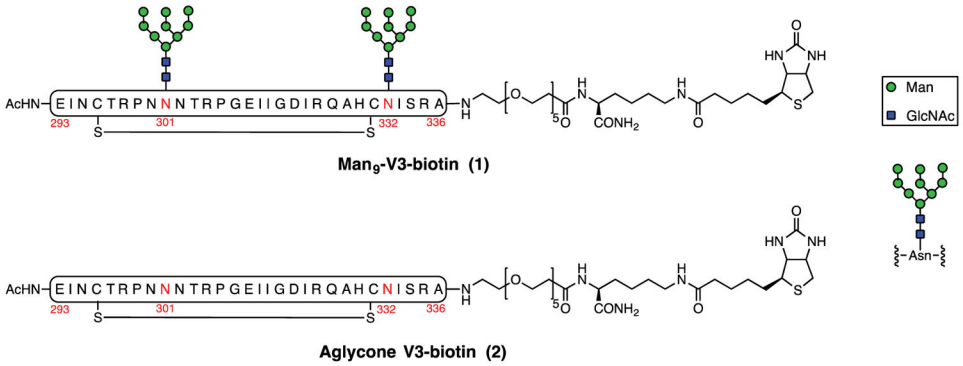

Fig. 1. Design of gp120 V3 domain broadly neutralizing epitope mimics

Structure of the chemically synthesized Man_9-V3-biotin glycopeptide and of aglycone V3-biotin. See procedures for synthesis in Supplementary Text and data set S1.

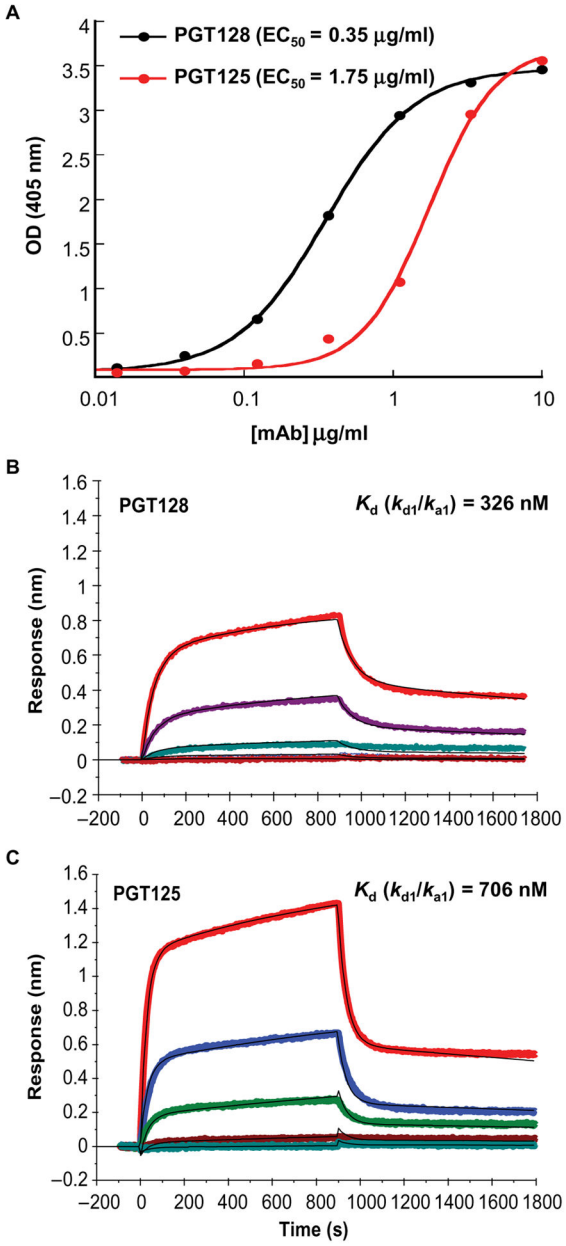

Fig. 2. Man_9-V3 glycopeptide binding to V3-glycan bnAbs PGT128 and PGT125

(**A**) ELISA binding analysis to calculate EC_{50} of PGT128 and PGT125 binding to Man_9-V3 glycopeptide. OD, optical density. (**B** and **C**) BLI binding analyses for K_d measurements for the binding of PGT128 (B) and PGT125 (C) to Man_9-V3 glycopeptide. Kinetics rates (k_{a1} and k_{d1}) of the faster components (figs. S7 and S8) were derived from global curve fitting analysis to a bivalent avidity model and used to derive the apparent K_d values. Binding analysis for affinity measurements was carried out by BLI, as described in Materials and Methods. Data are representative of three and two independent experiments, respectively, for PGT128 and PGT125.

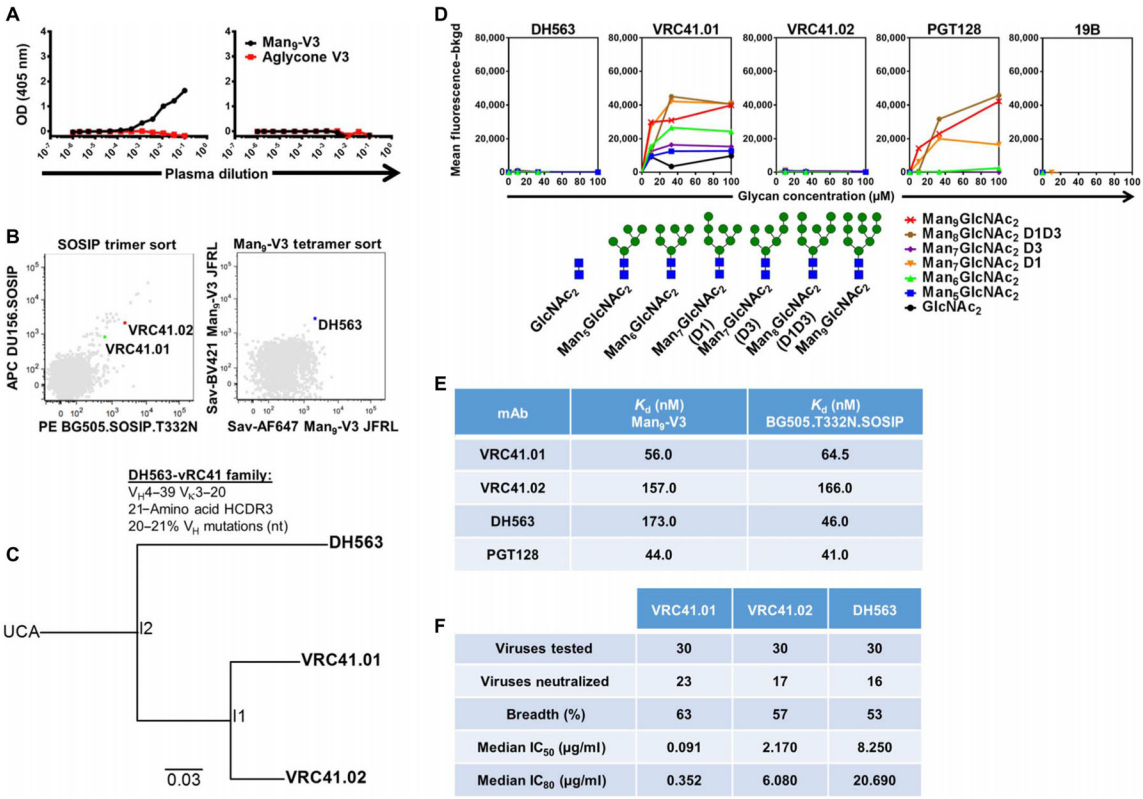

E

mAb	K_d (nM) Man_9-V3	K_d (nM) BG505.T332N.SOSIP
VRC41.01	56.0	64.5
VRC41.02	157.0	166.0
DH563	173.0	46.0
PGT128	44.0	41.0

F

	VRC41.01	VRC41.02	DH563
Viruses tested	30	30	30
Viruses neutralized	23	17	16
Breadth (%)	63	57	53
Median IC_{50} (μg/ml)	0.091	2.170	8.250
Median IC_{80} (μg/ml)	0.352	6.080	20.690

Fig. 3. Isolation and characterization of N^{332}-dependent antibodies isolated using native-like SOSIP trimers and synthetic Man_9-V3 glycopeptide

(**A**) ELISA binding analyses of plasma from the HIV-infected donor CH765 to Man_9-V3 and aglycone V3 peptides. Donor plasma was screened in duplicate assays, and binding is represented as mean values. (**B**) Memory B cells from donor CH765 were decorated with either fluorophore-conjugated BG505.T332N.SOSIP and DU156.12.SOSIP in phycoerythrin (PE) and allophycocyanin (APC), or Man_9-V3 tetramers tagged to SA–AF647 (Alexa Fluor 647) and SA–BV421 (Brilliant Violet 421). The B cells from which CH765-VRC41.01, VRC41.02, and DH563 were cloned are indicated as green, red, and blue dots, respectively. (**C**) Immunogenetics and phylogeny of the DH563-VRC41 clonal lineage were inferred using Clonanalyst (33, 34). See also fig. S3. nt, nucleotide. (**D**) Reactivity of CH765-VRC41.01, CH765-VRC41.02, and DH563 to Man_5, Man_6, Man_7-D1, Man_7-D3, Man_8-D1D3, and Man_9 glycans, depicted on the right, printed on an array and detected via immunofluorescence. See also figs. S5 and S6. (**E**) Affinity measurements of newly isolated V3-glycan mAbs to Man_9-V3 and BG505. T332N.SOSIP trimer were determined by BLI. Binding curves and data analysis are shown in figs. S7 and S8. (**F**) CH765-VRC41.01, VRC41.02, and DH563 were tested for neutralization breadth against a diverse panel of Env pseudoviruses using the TZM-bl assay. See also table S2 and fig. S9.

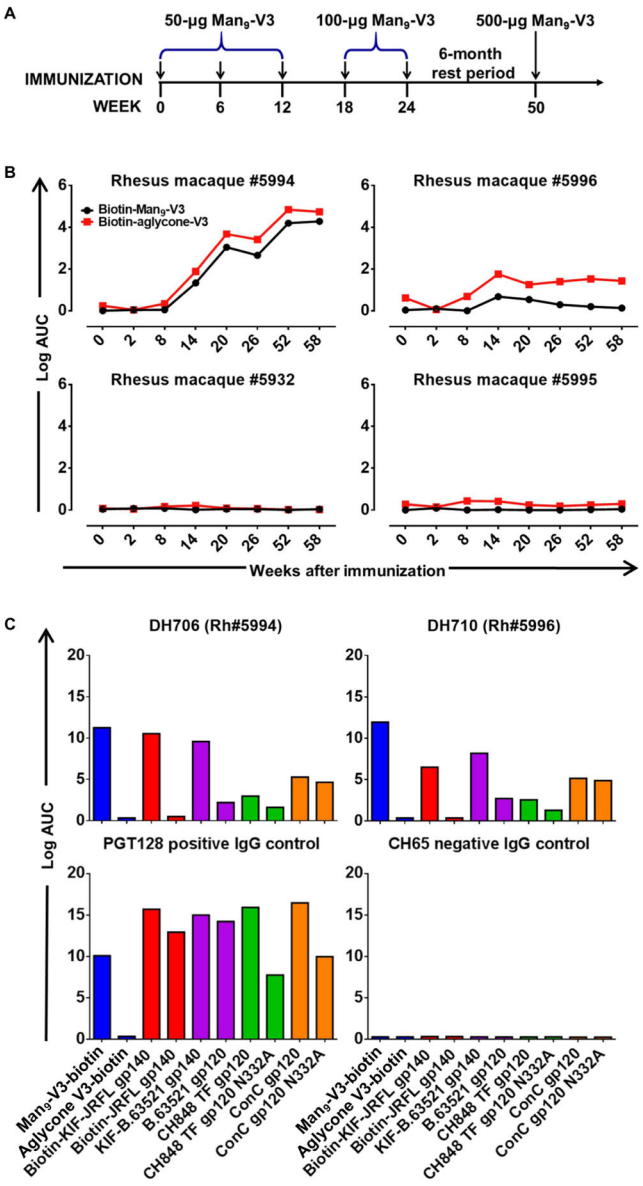

Fig. 4. Immunogenicity of Man_9-V3 glycopeptide in rhesus macaques

(**A**) Study design to assess immunogenicity of Man_9-V3 in rhesus macaques. Monomeric Man_9-V3 was formulated in GLA-SE adjuvant and injected intramuscularly in sequentially increasing doses, as indicated. (**B**) Plasma from immunized macaques was tested for binding to biotinylated Man_9-V3 and aglycone V3 in ELISA, as described in Materials and Methods. (**C**) Man_9-V3 reactive antibodies were isolated via antigen-specific memory B cell sorts and tested for binding to recombinant HIV-1 Envs in ELISA. See also fig. S11 and table S3. AUC, area under the curve.